ToF−SIMS Investigation of Octadecylphosphonic Acid Monolayers on a Mica Substrate

J. T. Francis,* H.-Y. Nie,* and N. S. McIntyre

Surface Science Western, Room G-1, Western Science Centre, The University of Western Ontario, London, Ontario N6A 5B7, Canada

D. Briggs

Centre for Surface Chemical Analysis, University of Nottingham, University Park, Nottingham NG7 2RD, United Kingdom

Received May 23, 2006. In Final Form: July 20, 2006

In this paper, time-of-flight secondary ion mass spectrometry (ToF−SIMS) under static conditions was used to investigate self-assembled monolayers (SAMs) of octadecylphosphonic acid (OPA) formed on freshly cleaved muscovite mica substrates. The coverage of OPA on mica ranged from 20 to 100%, with a film thickness of 1.7 ± 0.2 nm, which was determined by atomic force microscopy (AFM) imaging. The relative intensity of the specific secondary ion species associated with the OPA and with the exposed mica substrate exhibited good correlation with surface coverage. An excellent correlation was also observed ($R^2 = 0.98$) between the relative SIMS $[OPA\text{-}H]^-$ intensity and the surface carbon concentration (OPA C 1s, in atomic %) from XPS at the prescribed surface coverage. The observation of positive and negative OPA molecular attachment of secondary ions involving the substrate species is discussed in terms of the chemical affinity of the OPA phosphonate headgroup for the cleaved mica surface as well as the sampling depth. In addition, the OPA molecular attachment species formed with the potassium ions on the cleaved mica substrate dominated the positive secondary ion mass spectrum in the high-mass range. A temperature-dependent, ToF−SIMS study employing in situ heating of a 100% coverage OPA monolayer revealed that the molecules begin to diffuse above ∼80 °C, resulting in a decrease in the relative secondary ion yield of the OPA-specific secondary ions. This observation is hypothesized to be due to a decrease in the effective coverage of the substrate by the OPA molecules, which in turn could be due to the formation of multilayers upon heating in an effort to minimize the energy of the system. The interesting behavior of the novel OPA dimer species as a function of temperature is also reported. It was observed that the relative intensity of OPA and the mica-specific secondary ion peak intensities to that of Si (mica substrate) provides an effective means to estimate the change in coverage at elevated temperatures.

Introduction

Self-assembled monolayers (SAMs) on solid surfaces have generated tremendous interest as they are a basis for building two-dimensional, ordered molecular structures.[1] The potential technological applications for SAMS are particularly appealing, including nanolubricants for advanced micro-electromechanical systems and magnetic storage hard disks.[2,3] SAMS are typically characterized by their ease and reproducibility of preparation, chemical stability, and well-ordered character. As such, they are receiving increased attention in the literature as model systems for time-of-flight secondary ion mass spectrometry (ToF−SIMS) studies of thin organic layers under static conditions.[4−8] ToF−SIMS is especially suitable for probing elemental and molecular information from the topmost surface (one to three monolayers), for both inorganic and organic materials.[4] The most thoroughly studied SAMs to date are alkanethiols on gold and alkyltrichlorosilanes on oxide surfaces.[9−12]

In this paper, we report the results of ToF−SIMS and AFM analyses on octadecylphosphonic (OPA) SAMs on mica (muscovite) substrates, with the surface coverages ranging from 20 to 100% of a monolayer according to atomic force microscopy (AFM) imaging results. Note that this is a distinctly different SAM/substrate system than those previously studied.[13−16] In this case, the mica cleaves neatly into sheets, resulting in an atomically flat substrate. The absorption of the OPA onto mica is not yet well-understood. However, the ToF−SIMS results presented in this work provide insight into the nature of the interaction between the phosphonic acid headgroup of the OPA and the cleaved muscovite surface, through the examination of positive and negative OPA−mica attachment ions.

AFM results on OPA SAMs with varying surface coverage at room temperature (RT) are used as a gauge here to determine what level of correlation exists between the relative intensities of specific ion fragments characteristic of the OPA and the mica substrate from ToF−SIMS and the actual OPA SAM surface coverage. Furthermore, the results of these initial experiments provide a foundation to address the question as to what happens

* Corresponding authors. E-mail: (J.T.F.) jfranci2@uwo.ca and (H.-Y.N.) hnie@uwo.ca.

(1) Whitesides, G. M.; Mathias, J. P.; Seto, C. T. *Science* **1991**, *254*, 1312.
(2) Maboudian, R.; Ashurst, W. R.; Carraro, C. *Tribology Lett.* **2002**, *12*, 95.
(3) Choi, J.; Kawaguchi, M.; Kato, T. *J. Appl. Phys.* **2002**, *91*, 7574.
(4) Benninghoven, A. *Angew. Chem., Int. Ed.* **2003**, *33*, 1023.
(5) Delcorte, A.; Betrand, P.; Arys, X.; Jonas, A.; Wischerhoff, E.; Mayer, B.; Laschewsky, A. *Surf. Sci.* **1996**, *366*, 149.
(6) Textor, M.; Ruiz, L.; Hofer, R.; Rossi, A.; Feldman, K.; Hahner, G.; Spencer, N. D. *Langmuir* **2000**, *16*, 3257.
(7) Graham, D. J.; Ratner, B. D. *Langmuir* **2002**, *18*, 5861.
(8) Wong, S. C. C.; Lockyer, N. P.; Vickerman, J. C. *Surf. Interface Anal.* **2005**, *37*, 721.
(9) Nuzzo, R. G.; Allara, D. L. *J. Am. Chem. Soc.* **1983**, *105*, 4481.
(10) Maoz, R.; Sagiv, J. *J. Colloid Interface Sci.* **1984**, *100*, 465.
(11) Ulman, A. *Chem. Rev.* **1996**, *96*, 1533.
(12) Schreiber, F. *Prog. Surf. Sci.* **2000**, *65*, 151.
(13) Woodward, J. T.; Ulman, A.; Schwartz, D. K. *Langmuir* **1996**, *12*, 3626.
(14) Neves, B. R. A.; Salmon, M. E.; Russell, P. E.; Troughton, E. B., Jr. *Langmuir* **2000**, *16*, 2409.
(15) Schwartz, D. K. *Annu. Rev. Phys. Chem.* **2001**, *52*, 107.
(16) Nie, H.-Y.; Miller, D. J.; Francis, J. T.; Walzak, M. J.; McIntyre, N. S. *Langmuir* **2005**, *21*, 2773.

10.1021/la061456i CCC: $33.50
Published on Web 09/23/2006

to the OPA SAMS on the mica surface as a function of temperature. To this end, we have conducted an in situ heating experiment employing ToF−SIMS, wherein the temperature of a 100% initial surface coverage OPA SAM on the mica sample was incremented from −34 to 150 °C.

Experimental Procedures

Sample Preparation. A crystalline powder of OPA [$CH_3(CH_2)_{17}PO(OH)_2$] was obtained from Alfa Aesar (Ward Hill, MA). Samples of the OPA monolayer with various surface coverages up to 100% were prepared by a spin-coating OPA solution in chloroform onto freshly cleaved mica substrates, typically 1 cm × 1 cm in size, the details for which can be found elsewhere.[17]

AFM Methodology. A dynamic force AFM (TopoMetrix Explorer) was used to image the OPA layers formed on the mica substrate. Silicon cantilevers with a spring constant of ∼40 N/m were used. The cantilever was 125 μm long, 30 μm wide, and 3.7 μm thick. The radius of the tip attached to the free end of the cantilever was 10−20 nm. This sharp tip was used to probe the morphology of the sample surface. The surface morphology was obtained by keeping a constant damped amplitude of the oscillating cantilever between the tip and the sample surface, while the feedback system adjusted the distance between them.

ToF−SIMS Methodology. An ION-TOF (Gmbh), TOF−SIMS IV single-stage reflectron instrument with a 10 kV post acceleration was used to study the OPA SAMs prepared on the mica substrate. For all experiments, a 9 keV pulsed primary $^{133}Cs^+$ ion beam was used to bombard the sample surface in a rastered fashion, with a target current of 2 pA.

OPA Surface Coverage. A primary ion dose of 2×10^{12} ions/cm^2 was maintained for the surface coverage experiments by using fresh areas for each measurement. Both positive and negative secondary ion mass spectra were acquired from four replicate 200 μm × 200 μm areas at each OPA surface coverage. This series of experiments was performed with the samples at RT.

OPA Temperature Programming. For the in situ ToF−SIMS heating experiment, the sample was mounted in a custom stage that could either be cooled via intimate contact with a coldfinger utilizing liquid nitrogen and/or resistively heated. A Eurotherm 902 Precision Temperature Controller was employed to linearly ramp the sample temperature in situ from an initial value of −34 °C at a rate of 5 °C/min and hold it at various selected points to a final temperature of 150 °C. The estimated error in temperature measurement is <1% for this system. A 500 μm × 500 μm area was analyzed at selected incremental temperatures over the −34 to 150 °C range. The total primary ion dose was maintained $<7 \times 10^{11}$ ions/cm^2. Prior to measurement, a 200 μm × 200 μm crater was inscribed in the center of the 500 μm × 500 μm analysis area via a sharp boost in the primary ion beam pulse width for a few seconds while the beam was rastering. This was done to provide a reference feature in the ion images (extracted post-analytically from the raw data stream) that will be discussed later in terms of OPA mobilization temperature. Although the beam spot size of the primary Cs^+ beam was > 1μm, it was more than sufficient for the large area imaging required in this work. Finally, a pulsed, low-energy (18 eV) electron flood was employed to neutralize sample charging. The current was maintained below a ∼20 μA maximum to avoid sample damage.

Results and Discussion

OPA Surface Coverage. Shown in Figure 1 are AFM images for four OPA SAM samples with coverages of (a) 20%, (b) 50%, (c) 70%, and (d) 100%, prior to ToF−SIMS analysis. The surface coverage estimated from the AFM has an accuracy of ∼5%. The height of the OPA monolayers measured 1.7 ± 0.2 nm. The OPA on mica samples with varying surface coverages were obtained by choosing the appropriate solution concentration, relative humidity, and spin-casting speed. The 100% surface coverage OPA monolayer sample (see Figure 1d) shows a flat, featureless surface.

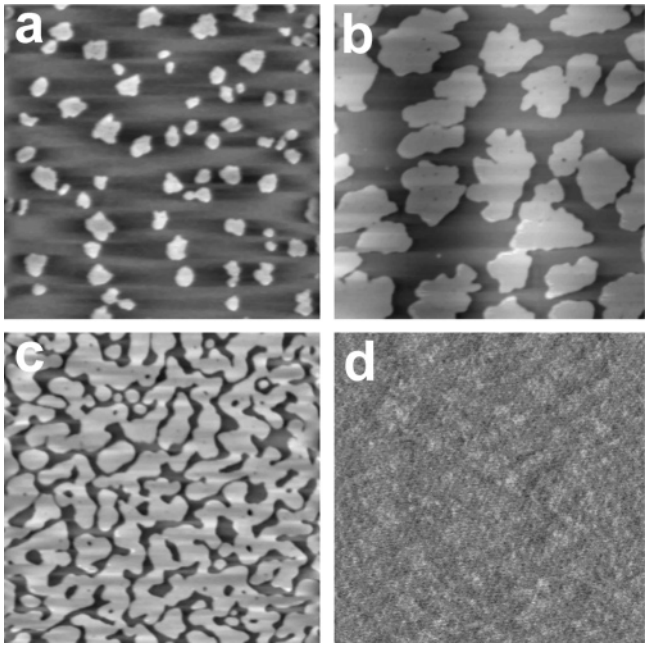

Figure 1. Gray scale AFM topographic images (scan area: 2 μm × 2 μm) of four different OPA samples prepared under appropriate conditions on a freshly cleaved muscovite with surface coverage (%) of (a) 20%, (b) 50%, (c) 70%, and (d) 100%. In panels a−c, the darker shading represents the substrate. The height range for panels a−c is 2.5 nm. The morphology in panel d has a height range of 0.3 nm, showing a featureless surface with a corrugation height of a couple of angstroms.

Shown in Figure 2 a−d is the positive secondary ion mass spectrum for the 100% coverage of the OPA/mica sample. In Figure 2a, the characteristic hydrocarbon series is representative of the long-chain alkane OPA tail. Note in particular that several elemental mica substrate constituents such as Al^+, Si^+, and K^+ are detected with rather significant intensity. Mica is somewhat unique here as a substrate (as compared to previous SAMs studies on thin metal layers) in that these elements can originate from different periodic layers in the mica structure. Mica consists of a stack of tetrahedral silicate units that are hexagonally linked to form sheets.[18−20] Every two silicate sheets sandwich an octahedral alumina [$AlO_4(OH)_2$] layer in between. In addition, the tetrahedral silicate sheets in mica are connected by rather weak K^+ ions, which are responsible for its facile cleaving behavior. Simplistically then, on a cleaved mica surface, there should remain hexagonally linked, tetrahedral oxygen groups with half the original number of K^+ ions distributed over it. Thus, the Al^+ that is detected originates at least 0.5 nm below the cleaved surface (i.e., the first layer) and quite possibly in a decreasing probability as a function of depth from the periodic $AlO_4(OH)_2$ structures. The same argument could be applied to the origins of K^+, which, in addition to sitting right at the cleavage plane upon which the OPA was adsorbed, has a periodicity of ∼1 nm between layers in muscovite mica.

A crude estimation of the attenuation in the positive and negative secondary ion yields for the mica-specific species can be made here, using the data for an OPA SAM thickness of 1.7

(17) Nie, H.-Y.; Walzak, M. J.; McIntyre, N. S. *J. Phys. Chem. B* **2006**, *110*, in press 10.1021/jp062811g.

(18) Gales, J. M.; Mahanti, S. D. *Phys. Rev. B* **1989**, *40*, 12319.

(19) Wada, N.; Kamitakahara, W. A. *Phys. Rev. B* **1991**, *43*, 2391.

(20) Ferraris, G.; Ivaldi, G. In *Micas: Crystal Chemistry & Metamorphic-Petrology*; Mottana, A., Sassi, F. P., Guggenheim, S., Eds.; The Mineralogical Society of America: Washington, DC, 2002; p 117.

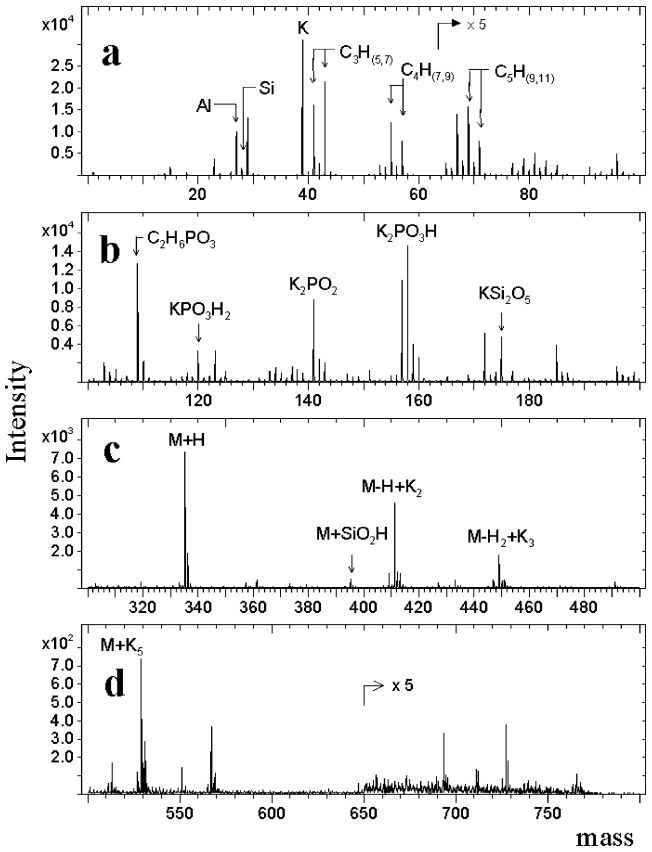

Figure 2. ToF−SIMS positive secondary ion mass spectra of a 100% surface coverage OPA SAM on a muscovite mica substrate.

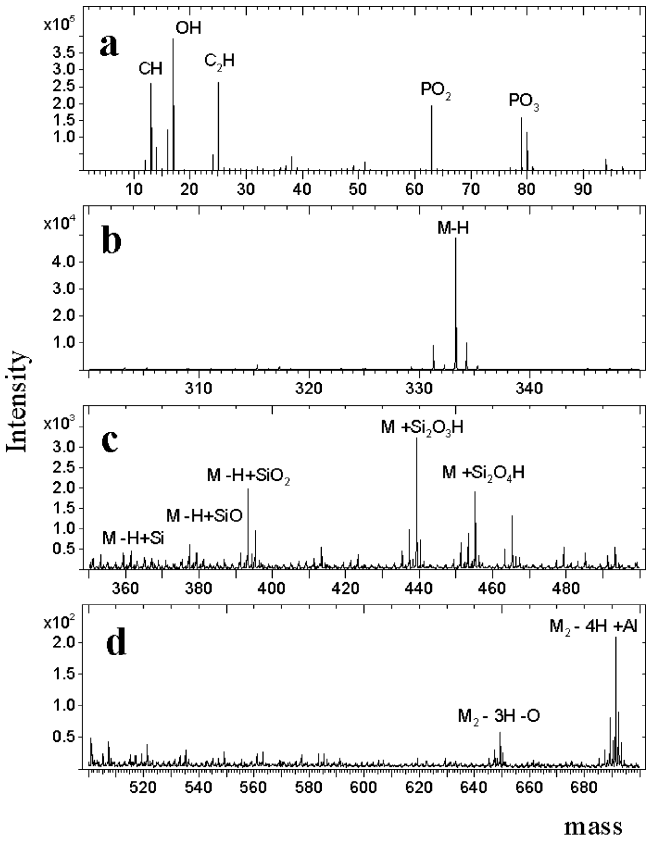

Figure 3. ToF−SIMS negative secondary ion mass spectra of a 100% surface coverage OPA SAM on a muscovite mica substrate.

± 0.2 nm (as determined via AFM) at 100% coverage and at 0% coverage (i.e., bare mica). It is found that the relative Si^+, K^+, and SiO_3H^- intensities from mica are diminished by 88, 80, and 78%, respectively, by a 1.7 nm OPA SAM. Delcorte et al. reported a 95% attenuation in the secondary ion intensity of Si^+ and SiO_3H^- fragments due to 4.5 and 1.5 nm, respectively, of a polymeric film on SiO_2.[5] The two situations differ in that the mica substrate is not homogeneous in composition with depth, whereas the SiO_2 is. The comparison strongly suggests, however, that the majority of the detected secondary ions from the mica substrate (both atomic and cluster types) must originate from the uppermost layer in which they exist.

Figure 2b reveals prominent secondary ions of a composition ($KPO_3H_2^+$, $K_2PO_2^+$, and $K_2PO_3H^+$) corresponding to the attachment of substrate potassium ions to the phosphonate portion of the OPA headgroup. It is possible that these species may originate as much larger, highly energetic, secondary parent ions with all or a large portion of the long-chain alkane tail group after the initial sputtering event. The relatively intense yield of these ions is also indicative of the strength of the interaction between the phosphonate group and the potassium ions on the mica surface. More specifically, the extremely high-ionization probability of potassium undoubtedly contributes to the strong positive secondary ion yield for the potassium-cationized phoshponate species. In our case, because the potassium ions exist on the cleaved mica surface onto which the OPA headgroups are anchored, it is both physically and chemically favorable for salt formation. Information about the interaction between the headgroup and the potassium ion is, in our opinion, apparently inaccessible by other analytical methods used to characterize OPA SAMs on a mica substrate.

Also seen in Figure 2b are ion fragments of composition $C_2H_6PO_3^+$ and $KSi_2O_5^+$, which unlike the attachment ions just described previously could likely arise solely from the OPA molecule and the mica substrate, respectively, during the initial sputter event. Again, however, they could also arise as subsequent fragmentation products of the larger, high internal energy, OPA−substrate attachment secondary ions.

Shown in Figure 2c is perhaps the most diagnostic OPA-specific secondary ion, $C_{18}H_{40}PO_3^+$ or $[M + H]^+$, while Figure 2d reveals higher mass, OPA molecular attachment species with mica substrate constituents such as $[M + SiO_2H]^+$, $[M - H + K_2]^+$, $[M - H_2 + K_3]^+$, and $[M + K_5]^+$. Note that these attachment ions have comparable intensities relative to $[M + H]^+$, especially $[M - H + K_2]^+$. This could suggest ionic interactions between the phosphonic acid headgroup and the potassium ions on the cleaved mica substrate. Therefore, our ToF−SIMS results clarify the important role played by the potassium ions left on the mica substrate upon cleavage.

Figure 3a shows primarily CH^-, C_2H^-, PO_2^-, and PO_3^- species, no doubt derived from the OPA hydrocarbon tail and phosphonate headgroup, respectively. Figure 3b reveals the very prominent deprotonated molecular ion $C_{18}H_{38}PO_3^-$, denoted as $[M - H]^-$, which is roughly an order of magnitude greater in intensity than the $[M + H]^+$ ion in Figure 2c. Figure 3c shows a series of OPA−substrate attachment ions of the form $[M - H_x + Si_yO_z]^-$. Interestingly, Figure 3d reveals dimer species, $[M_2 - 3H - O]^-$ and $[M_2 - 4H + Al]^-$. The assignment of the latter has been confirmed by accurate mass measurement, as well as a careful comparison to the results of the ToF−SIMS experiments on OPA SAMs formed on other substrates such as oxidized aluminum. It is intriguing that the dimer is associated with aluminum that is supposedly underneath the cleaved mica surface. This suggests a strong interaction between the phosphonic acid headgroup and the metal ion. As aluminum exists beneath the cleaved mica surface, these $[M_2 - 4H + Al]^-$ dimers thus could

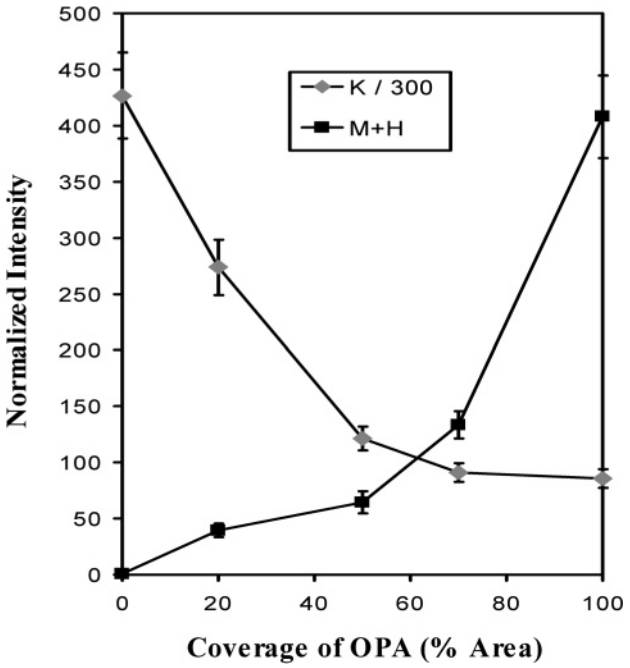

Figure 4. Plot of surface coverage of OPA on mica vs $[M + H]^+$ and K^+ intensities from ToF−SIMS measurements. Raw secondary ion intensities have been normalized to the total ion intensity using the ratio $I_{norm} = I_{raw}/I_{tot} \times 10^5$.

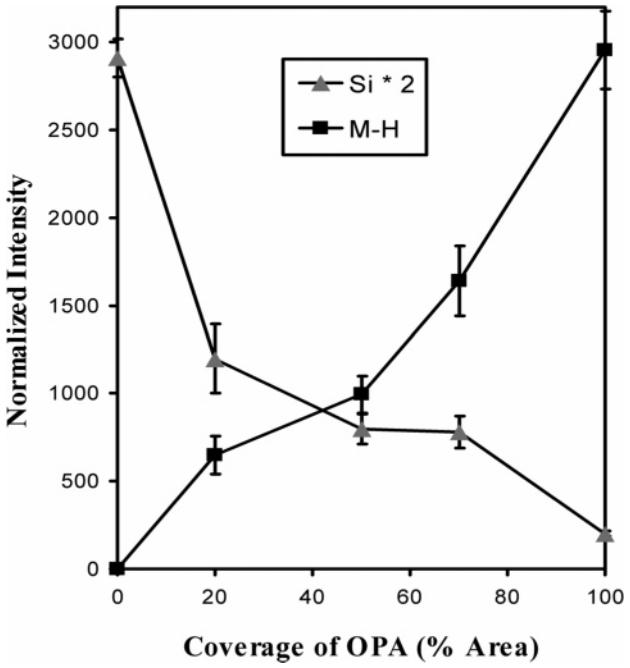

Figure 5. Plot of surface coverage of OPA on mica vs $[M - H]^-$ and Si^- intensities from ToF−SIMS measurements. Raw secondary ion intensities have been normalized to the total ion intensity using the ratio $I_{norm} = I_{raw}/I_{tot} \times 10^5$.

be formed during primary ion bombardment. Note that, by comparison, there does not appear to be any dimer species observed with any significant intensity in the corresponding positive ion mass spectra in Figures 2a−d.

Figures 4 and 5 plot the secondary ion peak intensities for $[M + H]^+$, $[M - H]^-$, K^+, and Si^- as a function of surface coverage on mica by OPA. The raw secondary peak intensities have been normalized to the total ion intensity and multiplied by 10^5. Figure 4 shows a relatively smooth increase in the $[M + H]^+$ intensity with a concomitant decrease in the K^+ signal (derived from the

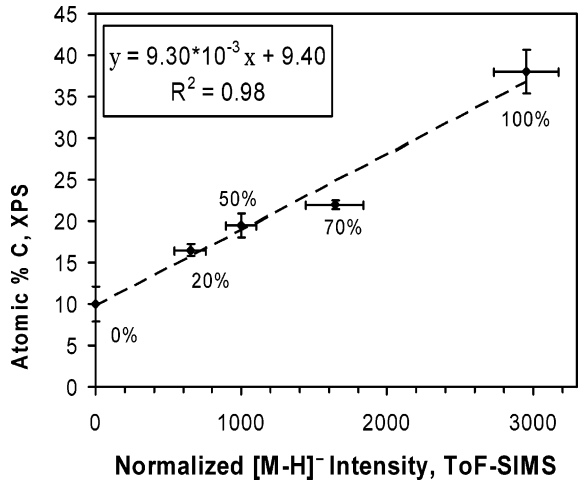

Figure 6. Correlation between atomic % C from XPS and normalized $[M - H]^-$ intensity from ToF−SIMS for identically prepared OPA on mica samples at various surface coverages (indicated below data points).

substrate mica cleavage plane) as a function of OPA SAM surface density. A similar trend is observed in Figure 5, following the $[M - H]^-$ deprotonated OPA molecular ion and Si^- from the mica substrate as a function of the OPA surface coverage.

In our earlier XPS study, we reported that the XPS carbon concentration increased linearly as a function of OPA coverage on identically prepared OPA on mica samples.[21] Therefore, we expected a good correlation between the XPS and the ToF−SIMS data. In particular, the ToF−SIMS normalized $[M - H]^-$ intensity was plotted against the XPS carbon concentration (in atomic %) at surface coverages of 0, 20, 50, 70, and 100% OPA; this is presented in Figure 6. The XPS work showed an unexpectedly low attenuation of the substrate signals by the OPA layer, and consequently, the carbon concentration is effectively a measure of OPA coverage.[21] Similarly, the normalized $[M - H]^-$ intensity will measure coverage if the yield is independent of lateral interactions within the SAM. Graham and Ratner reported a good linear correlation between their PCA-derived, ToF−SIMS SAM Ratio, which is at least in principle similar to the normalized $[M - H]^-$ intensity used here and the XPS [Au/C] ratio as a function of dodecanethiol SAM on gold-coated substrate coverage.[7] On the basis of our AFM images in Figure 1, and the trends in Figures 4 and 5, we would expect the same trends in the OPA SAM on the mica system when correlating ToF−SIMS and XPS data for mica-specific species. From the previous discussion, then, decisive evidence has been provided that ToF−SIMS may be used to quantitatively measure OPA SAM coverage on a substrate like mica.

OPA Temperature Programming. A sample of 100% coverage of OPA on a mica substrate was used for ToF−SIMS measurements at different temperatures in situ. It must be emphasized here that over the entire temperature range investigated here (−34 to 150 °C), no discernible rise in the main vacuum chamber pressure was observed (5×10^{-9} Torr). From the previous discussion, it was decided to monitor the negative secondary ion species, given the increased $[M - H]^-$ intensity relative to $[M + H]^+$ and the presence of intriguing, negative secondary ion dimers that could yield interesting results as a function of increasing substrate temperature. Figure 7 plots the normalized secondary ion peak intensities of Al^-, Si^-, $[M - H]^-$, and $[M_2 - 4H + Al]^-$ as a function of in situ substrate

(21) McIntyre, N. S.; Nie, H.-Y.; Grosvenor, A. P.; Davidson, R. D.; Briggs, D. *Surf. Interface Anal.* **2005**, *37*, 749.

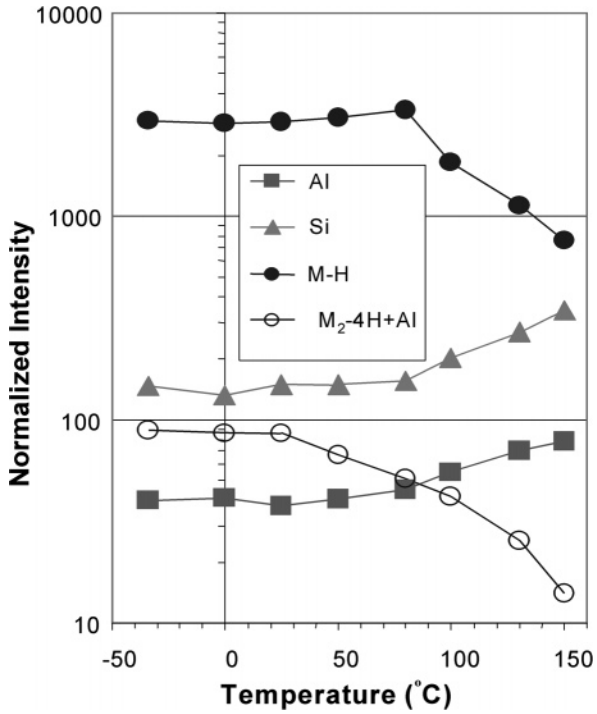

Figure 7. Plot of specific negative secondary ions as a function of temperature, for an initial 100% surface coverage of OPA on mica. Raw secondary ion intensities have been normalized to the total ion intensity using the ratio $I_{norm} = I_{raw}/I_{tot} \times 10^5$.

temperature. The $[M - H]^-$ peak intensity does not vary with temperatures up to 80 °C, which would suggest that the OPA SAM remains intact at 100% surface coverage. At temperatures higher than 80 °C, a relatively sharp decrease in the $[M - H]^-$ peak intensity is observed. In addition, the intensities of the substrate species Al^- and Si^- also appear stable with temperatures up to 80 °C, above which they begin to increase. The rate of increase of the substrate species intensities appears less dramatic than the concomitant decrease in $[M - H]^-$ intensity, however. Of particular interest is the trend in the dimer species, $[M_2 - 4H + Al]^-$ with temperature. The decay in its intensity transpires earlier in the temperature program than $[M - H]^-$ by comparison, just after 25° C. This observed trend in the dimer species $[M_2 - 4H + Al]^-$ intensity as a function of temperature was distinctly different from that for the monomeric species $[M - H]^-$. The $[M_2 - 4H + Al]^-$ intensity begins to fall off after 25 °C, which is well below the temperature at which the OPA SAMs is proposed to mobilize. We speculate that this intriguing behavior as a function of increasing temperature may be a consequence of formation of these species in the gas phase above the sample surface following primary ion bombardment, although the exact mechanism for the observed behavior remains unclear.

The mechanism for surface coverage decrease by the OPA SAMs on mica within the temperature range investigated here is not thought to be due to desorption of the OPA molecules because the melting point of OPA is ~100 °C. This has been confirmed by ex situ AFM investigation on annealing samples of OPA SAMs on mica at temperatures up to 200 °C.[14] In their study, Neves et al. observed aggregations of OPA molecules on the mica surface even after the sample had been heated to 200 °C.[14] Sheehan et al. have demonstrated that one can deposit OPA molecules on a mica surface at room temperature from a tip at a temperature of 122 °C on which the melted OPA acts as an ink.[22] These experimental results suggest that at these temperatures, OPA molecules will not desorb from the mica surface.

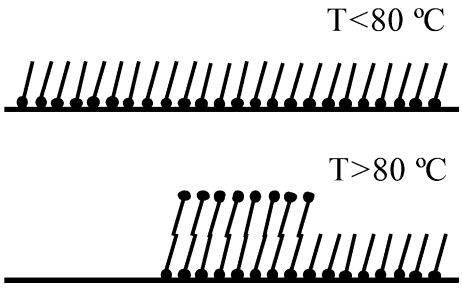

Figure 8. Schematic illustration for OPA molecular stacking (a simplified bilayer model) of a 100% surface coverage OPA monolayer on a mica substrate at elevated temperatures.

Neves et al. have also reported a stacking effect of OPA bilayers within a temperature range of 80−110 °C.[23] Their AFM images obtained on OPA multilayers on a mica substrate at 80 °C showed coalescence and stacking of two thick OPA layers. It is thus clear that OPA molecules as well as layers become mobile at temperatures above 80 °C. We here adopt the model of stacking the OPA molecules upon heating the substrate past 80 °C to explain our ToF−SIMS observations. This stacking scenario is presented in Figure 8 in a simplified model, where we only show the formation of bilayers. Under elevated temperatures (e.g., >80 °C), the molecules in the full-coverage SAMs cannot move laterally unless they flip over to form bilayer or multilayer stacks. This is the consequence of seeking the lowest possible energy configuration for the molecules when they are thermally excited. Therefore, detachment of the monolayer headgroups from the substrate will occur at elevated temperatures, and subsequent stacking of the layers will follow this event. Both the trends in the OPA- and mica-specific secondary ion species in Figure 7 are accommodated under this supposition. Thus, our ToF−SIMS results and the ex situ AFM results from Neves et al.[14] clearly showed a change in the OPA monolayer from ca. 80 °C. However, in situ AFM or other appropriate experiments under UHV conditions are needed to investigate the actual morphological change of the OPA monolayer on a mica substrate at elevated temperatures, from which one should obtain information about whether only a bilayer forms or multilayers also form.

To lend further credence to the OPA stacking hypothesis as well as providing at least a macroscopic view of the onset of OPA mobility at elevated temperatures beyond 80 °C, as shown in Figure 9, ion images of $[M - H]^-$ were extracted from the mass spectra raw data streams at each temperature during the entire −34 to 150 °C range. The images have a 128 × 128 pixel density and are presented on a color scale with lighter areas corresponding to regions of higher secondary ion intensity. Each image intensity has been auto-scaled by taking the minimum and maximum pixel intensities in each case and mapping them over a 0−255 increment color scale. The dark square in the center of each image is the sputter-etched crater described in the Experimental Procedures to provide a reference feature. Unless otherwise indicated, each image was acquired without delay after reaching the desired temperature. At −35 to 150 °C, it is emphasized here again that the total ion dose was maintained well below the static limit. Looking at Figure 9, the first four images ranging from −34 to 50 °C look essentially identical to the central sputter crater. The first image upon immediately reaching 80 °C does not appear to differ significantly from the previous four images at lower temperatures. However, after

(22) Sheehan, P. E.; Whitman, L. J.; King, W. P.; Nelson, B. A. *Appl. Phys. Lett.* **2004**, *85*, 1589−1591.
(23) Fontes, G. N.; Moreira, R. L.; Neves, B. R. A. *Nanotechnology* **2004**, *15*, 682.

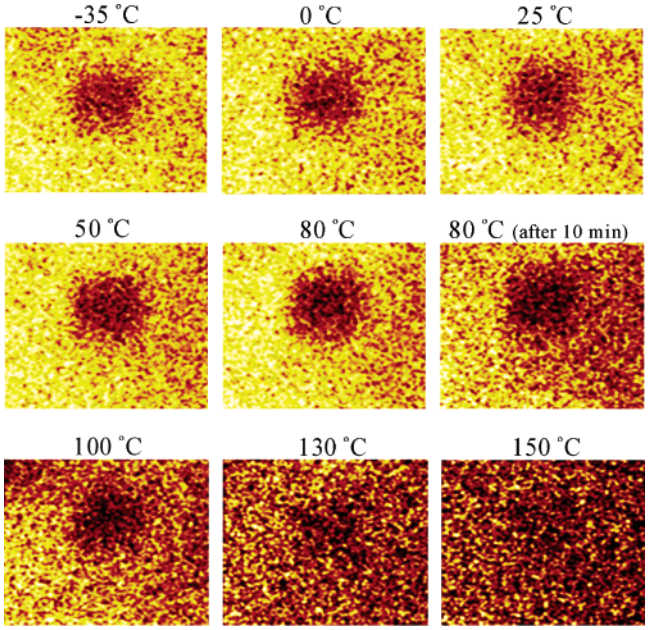

Figure 9. Ion images for $[M - H]^-$ as a function of substrate temperature. A rough, 200 μm × 200 μm crater exposing the substrate was created to provide a feature for reference in the images.

acquiring a second image at 80 °C following a delay for 10 min, one can see the onset of changes occurring in the ion image. In particular, the central sputter crater definition begins to become more diffuse, and there appears to be a darkening of a significant portion of the image. This suggests that the OPA mobilization occurs on a real time scale (i.e., seconds to minutes). Beyond 80 °C, the ion images continue to darken over larger proportions of the total imaged area as the temperature increase and the central sputter crater gradually become indistinguishable. At 100 °C, the crater is still recognizable. However, from 130 to 150 °C, the crater loses definition. This ToF−SIMS observation supports the in situ AFM results from Neves et al. that showed the OPA becoming liquid-like droplets.[23] At these temperatures, the OPA molecules become highly mobile, which renders the crater indistinguishable.

The trends described in Figure 9 can be ascribed to an OPA stacking hypothesis. As the OPA monolayers stack into domains of multilayers (Figure 8), an increasing proportion of the imaged area becomes exposed mica substrate. In addition, upon stacking of the OPA molecules, the secondary ion yield of the $[M - H]^-$ species may be attenuated relative to the original molecular surface configuration, with single OPA molecules adsorbed to the cleaved mica surface. Both of these factors could result in a lowering of the $[M - H]^-$ secondary ion yield over increasingly larger regions of the imaged area as the temperature increases.

On the basis of the previous OPA SAM surface coverage and temperature programmed ToF−SIMS results, one can estimate a quantitative change in surface coverage of 100% OPA SAM on a mica sample subjected to elevated temperatures. A plot of the ratio of the normalized $[M - H]^-$ secondary ion fragment intensity, both as a function of surface coverage and as a function of sample temperature (100% coverage sample only), is presented in Figure 10. An example is shown in Figure 10 by dotted lines, showing that the actual coverage at 130 °C is around one-half of the initial full coverage. The OPA stacking hypothesis at temperatures above 80 °C is invoked here again as the mechanism responsible.

Neves et al. have investigated the thermal stability of OPA SAM on a mica substrate by an ex situ AFM study.[14] From those

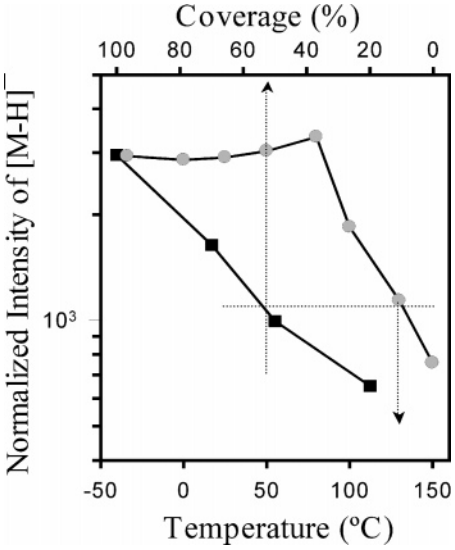

Figure 10. Plots of the normalized secondary ion intensity of $[M - H]^-$ vs OPA % area coverage (square) and vs temperature (circle, for the 100% coverage OPA on a mica substrate).

results, it was reported that OPA molecules start to become mobile from 90 °C. It was noted, however, that in contrast to the in situ heating ToF−SIMS experiments, the ex situ AFM experiments required cooling the sample back to room temperature after reaching the desired temperature. Thus, it may be a morphological difference between the OPA SAM samples analyzed via ToF−SIMS and those via AFM at a given temperature that could lead to the discrepancy in the OPA mobilization temperature.

Conclusion

In this work, we have employed ToF−SIMS under static conditions to characterize self-assembled monolayers (SAMs) of octadecylphosphonic acid (OPA) formed on mica (muscovite) substrates. A crude estimation of the attenuation in the positive and negative secondary ion yields for mica-specific species was made, using the data for an OPA SAM thickness of 1.7 ± 0.2 nm at 100 and 0% coverages. It was found that the relative Si^+, K^+, and SiO_3H^- intensities from mica are diminished by 88, 80, and 78%, respectively, by the OPA SAM.

Analysis of the positive secondary ion spectrum for a 100% coverage OPA SAM on mica revealed that the most diagnostic OPA-specific secondary ion was $C_{18}H_{40}PO_3^+$ or $[M + H]^+$. In addition, several intriguing OPA molecular attachment species with mica substrate constituents ($[M + SiO_2H]^+$, $[M - H + K_2]^+$, $[M - H_2 + K_3]^+$, and $[M + K_5]^+$) were observed with decent intensities relative to $[M + H]^+$. This suggests ionic interactions between the phosphonic acid headgroup and the potassium ion on the cleaved mica substrate. Analysis of the corresponding negative secondary ion spectrum for a 100% coverage OPA SAM on mica revealed the very prominent deprotonated molecular ion, $C_{18}H_{38}PO_3^-$ or $[M - H]^-$, which was roughly an order of magnitude greater in intensity than the $[M + H]^+$ ion. A series of interesting OPA−substrate attachment ions of the form $[M - H_x + Si_yO_z]^-$ was also observed. Unique dimer species, $[M_2 - 3H - O]^-$ and $[M_2 - 4H + Al]^-$, at relatively high masses were detected with nontrivial intensities. It was noted that, by comparison, there did not appear to be any such dimers in the positive secondary ion spectrum.

Using AFM results on OPA SAMs with varying surface coverage at room temperature as a gauge, a good correlation was found to exist between the percent OPA SAM surface coverage and the relative intensities of specific ion fragments that are

characteristic of the organic monolayer (i.e., $[M - H]^-$) and the mica substrate. In addition, utilizing XPS results from identically prepared OPA SAM samples, an excellent correlation was also observed ($R^2 = 0.98$) between the relative SIMS $[M - H]^-$ intensity and the surface carbon concentration (OPA C 1s, in atomic %) from XPS at the prescribed surface coverage.

Temperature programmed experiments were conducted by incrementing the sample temperature of a 100% surface coverage OPA SAMs sample from −34 to 150 °C. A change in the relative intensity of specific OPA and substrate fragments was observed beyond ∼80 °C as a function of increasing temperature. On the basis of these ToF−SIMS observations, we believe that the formation of OPA multilayers (including bilayers) beyond ∼80 °C could account for the observed decrease in coverage as a function of increasing temperature. We also showed that one may be able to estimate the effective coverage at elevated temperatures for a 100% coverage OPA SAM on a mica substrate by comparing the deprotonated molecular secondary ion intensity with the data obtained for known coverage OPA SAMs on a mica substrate.

LA061456I